On the Arrangement of the Micro-crystals in Rolled Platinum Plate. Part II

AUTHOR(S):

Tanaka, Shinsuke

CITATION:

Tanaka, Shinsuke. On the Arrangement of the Micro-crystals in Rolled Platinum Plate. Part II. Memoirs of the College of Science, Kyoto Imperial University. Series A 1925, 9(3): 197-217

ISSUE DATE:

1925-11-15

URL:

http://hdl.handle.net/2433/256750

On the Arrangement of the Micro-crystals in Rolled Platinum Plate. Part II.

By

Shinsuke Tanaka.

(Received August 1, 1925)

ABSTRACT.

The arrangement of micro-crystals in a thin platinum foil, which was prepared by rolling always in one and the same direction, was examined by x-rays. The arrangement of the micro-crystals in such foils is nearly similar to that described in the previous paper, where the foil was prepared by rolling alternately in opposite directions. But it is not entirely the same, the normal to the trapezohedral face of the micro-crystals is not, now, arranged exactly parallel to the direction of rolling, but inclined in the plane containing the direction of rolling and the normal to the rolled surface at an angle of about 10 degrees to the direction of rolling. This inclination seems to be opposite on the front and the back surfaces of the foil.

In his previous experiment,[1] the writer determined the arrangement of the micro-crystals in a rolled platinum plate prepared by rolling alternately in opposite directions. In the present experiment, he employed samples prepared by rolling always in one and the same direction. Using the same apparatus and under the same conditions as before, he obtained the X-ray interference figures reproduced in Fig. 1 of Plate I and represented diagramatically in Fig. 1′, by letting a narrow pencil of the X-rays from a molybdenum target strike normally the rolled surface of the specimen. In Fig. 1′ the direction parallel to that of rolling is represented by the arrow. Here it must be noted that the direction in which the process of rolling advances in the foil is expressed by the "direction of rolling." The thickness of the foil examined was about 0·04 m.m. As is seen from this figure, the intensity of the radiating bands is not the same now, on both sides of the horizontal bands, contrary to the former

1 These Memoirs, **8**, 319, (1925).

case, and the radiating bands in the upper half are more predominant than those in the lower half, as is seen in Fig. 1 of Plate I.

Fig. 1′.

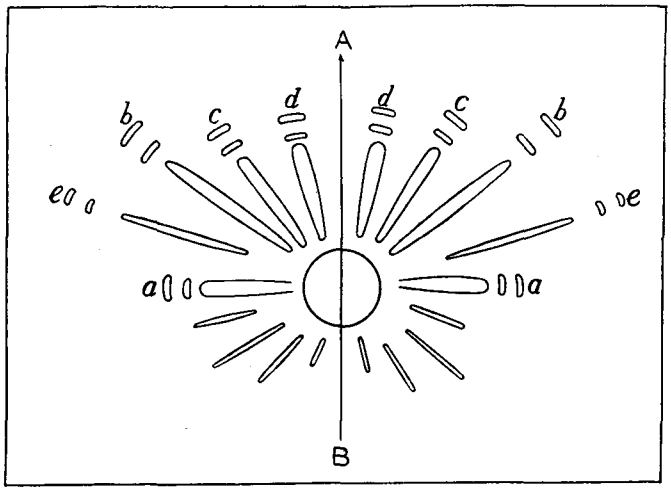

With respect to the distribution of the radiating bands, a slight difference from the former case was observed in the angles between the bands, and a new faint radiating band appeared now in the position 75°30′ from the direction of rolling. The observed values of the angles φ between the line BA, which is parallel to the direction of rolling, and the lines connecting the central spot and the positions of the spectra of the K_α doublet of molybdenum are given in the second column of the following Table 1.

Table 1.

Radiating Bands	Observed values of φ	Indices of faces	Calculated values of φ		
			$\alpha=90°$	$\alpha=80°$	$\alpha=75°$
a	91° 30′	$11\bar{1}$	90°	91° 30′	92°
b	55°	110	53° 30′	55° 30′	56°
c	35° 30′	001	34°	35° 50′	35° 30′
d	17° 50′	111	17° 30′	19° 30′	18° 30′
e	75° 30′	$13\bar{1}$ & $31\bar{1}$	75°	77° 30′	78° 30′

In the former case the distribution of the radiating bands was explained by considering that the normals of the planes (211) of the micro-crystals are arranged parallel to the direction of rolling in the foil, and the planes (110) containing these normals are nearly parallel to the rolled surface for the majority of the micro-crystals in the foil. If so, the trigonal axes in the planes (110) of the micro-crystals which are perpendicular to the normals of the planes (211) must be arranged perpendicularly to the direction of rolling in the rolled surface for the majority of the crystals. Now in the present case the circumstances are a little different, and the writer assumed that the normals to the planes (211) are not arranged exactly parallel to the direction of rolllng, but slightly inclined to the direction of rolling in the plane containing the direction of rolling and the normal to the rolled surface. Now let α be the angle between the incident beam of the X-rays and the normal of the plane (211), and Φ be the angle between the beam and the trigonal axis of the crystal which is perpendicular to the normal of the planes (211). Then the glancing angles θ for various reflecting planes and for various values of α and Φ will be calculated from equations (6) and (5) of the former paper. The results of calculation are tabulated in Tables 2, 3, 4 and 5.

It was stated in the former paper that the intensity, on the photographic plate, of the diffracted X-ray beam from a certain plane will be very weak when the glancing angle θ is too great. Thus by picking up only the small values of θ from the Tables, we can easily deduce some conclusions from these Tables.

When α does not differ very much from 90°, for example when it is 85°, as is seen from Table 3, the reflection of the X-ray from the planes 001, 110, 111 and 11$\bar{1}$ will occur in both cases when Φ is greater or smaller than 90°, and the intensity distribution of the interference bands obtained in this case will be nearly the same as that in the case when $\alpha=90°$, and there will be no reflection from the other crystal faces on account of the great values of θ. When α becomes much smaller, and if it is equal to 80° or 75°, it will be seen from Tables 4 and 5 that the following phenomena will take place : —

1. The reflection of the X-rays from the faces 001 will much stronger when Φ is smaller than 90°, and it will be much weaker when Φ is greater than 90°.

Table 2.

The values of θ ($\alpha=90°$).

Planes	β \ Φ	60°	70°	80°	90°	100°	110°	120°
001	35° 20′	17°	11°	6°	0°	6°	11°	17°
010	65° 55′	19°	28°	35°	45°	51°	60°	66°
100	65° 55′	66°	60°	51°	45°	35°	28°	19°
110	54° 45′	24°	16°	8°	0°	8°	16°	24°
$\bar{1}$10	90°	61°	70°	73°	90°	73°	70°	61°
101	30°	26°	28°	29°	30°	29°	28°	26°
$\bar{1}$01	73° 15′	58°	49°	39°	30°	20°	11°	2°
011	30°	26°	28°	29°	30°	29°	28°	26°
0$\bar{1}$1	73° 15′	2°	11°	20°	30°	39°	49°	58°
111	19° 20′	10°	7°	3°	0°	3°	7°	10°
$\bar{1}$11	61° 50′	63°	62°	57°	55°	46°	41°	33°
1$\bar{1}$1	61° 50′	33°	41°	46°	55°	57°	62°	63°
11$\bar{1}$	90°	30°	20°	10°	0°	10°	20°	30°

Table 3.

The values of θ ($\alpha=85°$).

Planes	β \ Φ	60°	70°	80°	90°	100°	110°	120°
001	35° 20′	19°	7°	2°	4°	10°	16°	21°
010	65° 55′	17°	26°	34°	42°	49°	55°	60°
100	65° 55′	69°	63°	59°	48°	39°	30°	21°
110	54° 45′	27°	19°	11°	3°	4°	13°	21°
$\bar{1}$10	90°	60°	70°	79°	90°	79°	70°	59°
101	30°	25°	33°	34°	35°	34°	33°	30°
$\bar{1}$01	73° 15′	63°	46°	37°	28°	14°	9°	0°
011	30°	26°	23°	25°	25°	32°	23°	21°
0$\bar{1}$1	73° 15′	2°	12°	22°	32°	33°	51°	60°
111	19° 20′	14°	11°	8°	5°	1°	2°	5°
1$\bar{1}$1	61° 50′	35°	44°	52°	59°	64°	67°	66°
$\bar{1}$11	61° 50′	56°	57°	55°	51°	45°	38°	30°
11$\bar{1}$	90°	30°	20	10	0	10	20	30°

Table 4.

The values of θ ($\alpha = 80°$).

Planes	β \ Φ	60°	70°	80°	90°	100°	110°	120°
001	35° 20′	8°	3°	2°	8°	14°	20°	25°
010	65° 55′	14°	22°	31°	39°	45°	51°	55°
100	65° 55′	74°	67°	59°	50°	41°	32°	22°
110	54° 45′	31°	22°	14°	6°	2°	10°	18°
$\bar{1}10$	90°	58°	67°	75°	82°	75°	68°	58°
101	30°	35°	38°	39°	40°	39°	38°	35°
$\bar{1}01$	73° 15′	51°	43°	35°	26°	17°	8°	2°
011	30°	16°	18°	19°	20°	19°	18°	16°
$0\bar{1}1$	73° 15′	4°	13°	23°	33°	42°	52°	63°
111	19° 20′	20°	16°	13°	9°	6°	3°	0°
$1\bar{1}1$	61° 50′	37°	46°	55°	63°	68°	71°	70°
$\bar{1}11$	61° 50′	51°	52°	50°	46°	40°	34°	26°
$11\bar{1}$	90°	30°	20°	10°	0°	10°	20°	30°

Table 5.

The values of θ ($\alpha = 75°$).

Planes	β \ Φ	60°	70°	80°	90°	100°	110°	120°
001	35° 20′	4°	1°	6°	12°	18°	24°	30°
010	65° 55′	11°	20°	27°	35°	41°	47°	50°
100	65° 55′	79°	70°	62°	52°	43°	33°	24°
110	54° 45′	34°	25°	17°	9°	1°	7°	15°
$\bar{1}10$	90°	56°	65°	72°	76°	72°	65°	55°
101	30°	40°	43°	45°	45°	45°	43°	40°
$\bar{1}01$	73° 15′	48°	41°	33°	24°	15°	6°	4°
011	30°	11°	13°	14°	15°	14°	13°	11°
$0\bar{1}1$	73° 15′	5°	15°	24°	34°	43°	54°	63°
111	19° 20′	24°	21°	18°	14°	11°	7°	4°
$1\bar{1}1$	61° 50′	36°	48°	57°	66°	73°	77°	74°
$\bar{1}11$	61° 50′	46°	47°	45°	42°	37°	30°	23°
$11\bar{1}$	90°	30°	20°	10°	0°	10°	20°	30°

2. The reflection from the faces 110 and 111 will be much stronger when Φ is greater than 90°, and it will be much weaker when Φ is smaller than 90° with X-rays of longer wave lengths.
3. The faces 11$\bar{1}$ reflect the X-rays equally in both cases when Φ is greater or smaller than 90°, as in the case of $\alpha=90°$.
4. The intensity of the reflected rays from the faces $\bar{1}$01 and 0$\bar{1}$1 will, even if they should appear, be very weak, because the value of θ is rather large in the neighbourhood of $\Phi=90°$ and becomes small only in the neighbourhood of 120° and 60° respectively.
5. The reflection from the faces 011 will only occur for X-rays of longer wave lengths when α becomes smaller.
6. There will be no reflection from other crystal faces on account of the great values of θ.

In the previous report, where the rolling was done alternately in opposite directions, two orientations of the micro-crystals as represented in Fig. 5 and Fig. 6 were considered to be the ideal ones. Now let the orientations represented by Fig. 2 and Fig. 3 be such two ideal orientations of the micro-crystals in the present case. When the foil was placed in a position perpendicular to the beam of the X-rays the value of α was 90° in the previous case, but it is a little different now. For the present, let us take 80° or 75° as the value of α, and see what will be the consequence of such an assumption.

When $\overrightarrow{QR}$, $\overrightarrow{QP}$ and $\overrightarrow{QL}$ are taken as positive directions of the x, y, z axes respectively, the faces 001, 111, 11$\bar{1}$ and 110 are represented by LMNK, KMS, KMQ and KMRP respectively in Figs. 2 and 3. The directions of the beam of the X-rays are represented by the arrows in Fig. 2 and Fig. 3. These directions are nearly, though not exactly as in the previous case, parallel to $\overrightarrow{MK}$ or $\overrightarrow{KM}$ in the present case. For the trigonal axis LS, which is perpendicular both to the normal QO of the face (211) and to the direction of the X-rays in the ideal orientation as represented in Fig. 2 and Fig. 3, the direction $\overrightarrow{LS}$ is taken as positive in accordance with our previous calculation. Therefore, when the crystals are rotated clockwise a little around the common axis as represented by the arrow, the value of Φ will become greater for the crystal represented by Fig. 2, and will become smaller for the crystal represented by Fig. 3. When the rotation is counter-clockwise the change of the values of Φ will be opposite. Now from Table 4 it will be seen that, when $\alpha=80°$ and $\Phi=90°$, the glancing angles θ are 8°, 9°, 0° and 6° for the faces 001, 111, 11$\bar{1}$ and 110 respectively. The positions of the interference spots

Fig. 2.

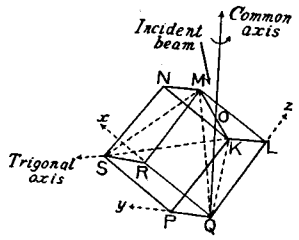

Fig. 3.

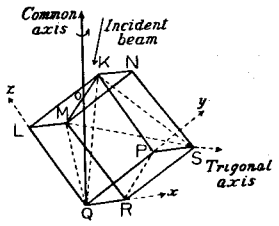

Fig. 4.

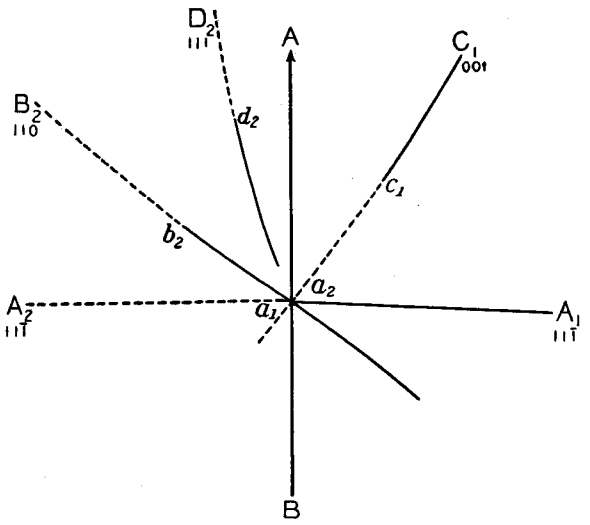

Fig. 5.

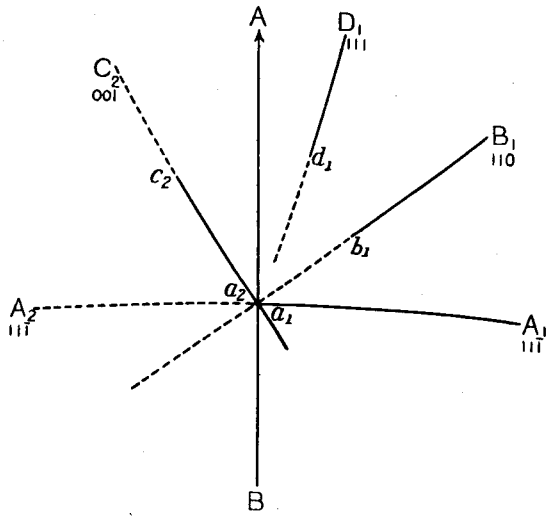

caused by the reflection of the X-rays from the crystal faces in the above orientations are calculated and represented in Figs. 4 and 5, by the points c_1, c_2, d_1, d_2, a_1, a_2, b_1 and b_2 respectively. When the crystals are rotated around the common axis, the interference bands will start from these points instead of from the central spot. The curves drawn in full lines in Fig. 4 represent the interference bands obtained when the crystal represented by Fig. 2 is rotated clockwise. If the rotation is counter-clockwise the interference bands represented by dotted lines in Fig. 4 will be obtained. Similarly the curves drawn in full and dotted lines in Fig. 5 are obtained by rotating respectively clock-wise and counter-clockwise

Fig. 6.

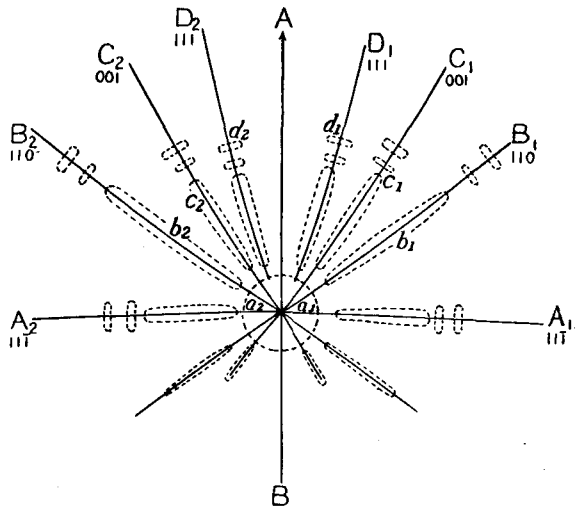

the crystals represented by Fig. 3. If the micro-crystals in the samples are situated in all the above positions, the interference figure with such foil will be obtained by superposing these two figures. If we suppose, as before, that for the majority of the micro-crystals the values of Φ are nearly equal to 90°, and that the number of the micro-crystals becomes smaller as the deviation of Φ from 90° becomes greater, then the intensity of the interference bands will be much stronger in the neighbourhood of the points c_1, c_2, d_1, d_2, a_1, a_2, b_1 and b_2 than in the other parts. The curves represented in Fig. 6 will show this consideration more clearly. In this case α was taken to be 80°, and the curves drawn in full lines represent the loci of the reflected X-ray beam corresponding to various values of Φ ranging between 70° to 110°. Therefore, when the common axis QO is not perpendicular to the incident beam but is inclined at an

angle of 80° or 75°, all the interference figures appearing on one side of the horizontal line will be much stronger than the other half, so far as the four predominant reflecting faces above mentioned are concerned; because the starting points of the curves, which correspond to the ideal orientation of the micro-crystals in the foil, are situated on one side of the horizontal line. It will easily be understood, from the figures from Fig. 2 to Fig. 5 that the side on which the common axis QO makes an acute angle with the incident beam, is the same as that on which the intensities of the interference figures are stronger.

Fig. 7.

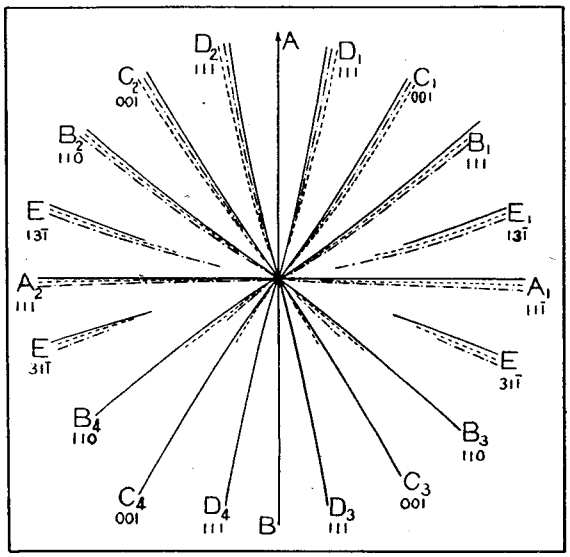

Since the values of β for the four faces above mentioned are known, the angular distribution of the interference bands caused by these four faces can be calculated for a given value of α, by equations (2), (3) and (4) in the previous report. The values of φ thus calculated for the K_α doublet of molybdenum are given in the fourth column of Table 1. The faces $\bar{1}01$ and $0\bar{1}1$ are represented by the planes MNQP and KNQR in Fig. 2 and Fig. 3. The interference figure corresponding to these planes, if it appeared, would be very weak for the reason stated before. This is in accordance with actual observation, and the writer could not detect the presence of any such interference band. It has already been stated that an interference band of very weak intensity marked by e in Fig. 1′ was detected on the photograph. The reflecting atomic plane corresponding to

this band was seen to be the face (311) of the crystals by the position of the spectrum of the K_α and K_β lines of molybdenum. By assuming the value of α to be 80°, and calculating the values of θ and φ corresponding to various values of Φ, it was seen that the interference band should appear on the upper side of the horizontal band, and that the value of φ for K_α line of molybdenum was in fair agreement with the observed one, as is seen in Table 1.

Fig. 7 represents the positions of the interference bands theoretically obtained by the above consideration. Here the curves drawn in full lines represent the bands obtained in the case when $\alpha=90°$ i. e. when the common axes of the micro-crystals are parallel to the direction of rolling, and the curves drawn in dotted lines and chain lines represent the interference bands obtained in the cases when $\alpha=80°$ and 75° respectively. For the values of Φ, all possible values ranging between 70° and 110° were taken in all the three curves. It will easily be seen from this figure that the curves drawn in dotted lines and those in chain lines are not much separated from those drawn in full lines in spite of there being such a considerable difference in the value of α as 10° or 15°, and the maximum deviation in the value of φ is only about 2°30′. In Fig. 6, the curves drawn in broken lines are a sketch of the outlines of the interference bands represented in Fig. 1′ and the curves drawn in full lines are the loci of the X-ray beam reflected from various faces of the crystals when $\alpha=80°$, and corresponding to various values of Φ ranging between 70° to 110°. As the coincidence between the observed and calculated positions of the interference bands seems to be rather satisfactory, the writer tried to see whether the consideration above mentioned will also account for the observations in various other respects.

Fig. 8.

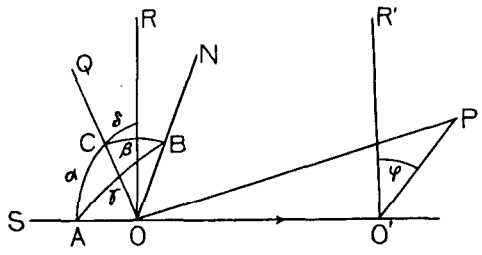

From the above consideration and by comparing the observed values of φ with those calculated, we know that the radiating bands a, b, c and d, in Fig. 1′ are caused by the reflection from the faces $11\bar{1}$, 110, 001 and 111 respectively. Thus from the observed values of φ corresponding to each reflecting face above mentioned, we can calculate the provable value of the inclination of the common axis of the micro-crystals from the direction of rolling.

In Fig. 8 OR represents the direction of rolling, ON the normal to a reflecting plane of the micro-crystals, and OQ the common axis. The X-ray beam proceeds along SO and is reflected toward OP. The angles $<$NOQ, $<$SON, $<$SOQ and $<$R′O′P are represented by β, γ, α and φ respectively. Then we have the following equation from the spherical triangle ABC,

$$\cos\beta=\cos\alpha\cos\gamma+\sin\alpha\sin\gamma\cos\varphi,$$

hence we have

$$\cos\alpha=\frac{\cos\beta\cos\gamma\pm\sin\gamma\cos\varphi\sqrt{\sin^2\gamma\cos^2\varphi+\cos^2\gamma-\cos^2\beta}}{\cos^2\gamma+\sin^2\gamma\cos^2\varphi}.$$

The observed value of φ and the values of α calculated from the above equation for each spectrum appearing at the end of each radiating band are tabulated in the following Table 6. As is given in the last

Table 6.

Radiating Bands	Indices of faces	Observed values of φ	Calculated values of α
a	$11\bar{1}$	91° 30′	80° 40′
b	110	55°	48° 45′ or 83 50′
c	001	35° 30′	75° or 82°

column of Table 6 we have two values of α for the spectrum at the end of each radiating band. But, as the values of α must be the same for every spectrum, we have taken 80°40′, 83°50′ and 82° as the values of α corresponding to the bands *a*, *b* and *c* respectively. The mean of these values is 82°10′. No reliable value of α can be obtained from the observed values of φ for the spectrum at the end of the band *d*, because the value of $\frac{d\varphi}{d\alpha}$ for that spectrum is small. Thus the values of α obtained from this spectrum was omitted in Table 6. As the provable value of α now obtained is 82°10′, the provable value of the inclination of the common axis from the direction of rolling is $90°-82°10'=7°50'$.

It has already been stated that when the rolling is done in the upward direction, the intensity of the interference bands becomes much stronger in the upper side than in the lower side as is denoted in Fig. 1′. Therefore the relative inclinations between the X-ray, the direction of rolling and the common axis of the micro-crystals will be as represented in Fig. 9.

If our consideration is correct, the difference in the intensity of the interference bands on both sides will be reversed when the X-ray is projected to the surface of the sample normally from the opposite direction. But the writer observed, on the contrary, that the intensity in the upper side was also much stronger than that in the lower side. Judging from this, it seems to be natural to consider that the foil is composed of two layers, and that in these two layers the common axes are inclined in opposite directions to the direction of rolling, as shown in Fig. 10. In this figure the direction of rolling is represented by the arrow. When the X-ray is projected normally to the rolled surface of the foil from the left side, the interference bands caused by the front layer A in Fig. 10 will predominate on the lower side, and those caused by the back layer B will predominate on the upper side of the horizontal line. The X-rays diffracted from the layer A must travel a longer path

Fig. 9.

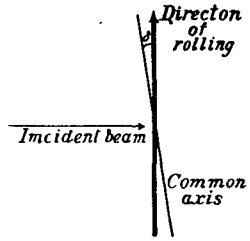

Fig. 10.

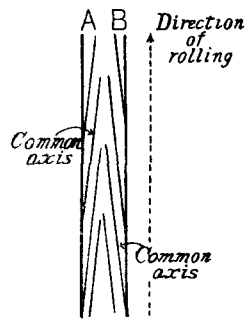

in the foil and consequently they will be much more absorbed than those diffracted from the layer B, due to the pretty large absorption coefficient of platinum. Thus the interference figure on the photograph will mainly be impressed by the X-rays diffracted from the back layer B of the foil, and the interference bands on the upper side of the horizontal line will be much stronger than those on the lower side. Similarly when the X-rays are projected in the opposite direction, i. e. from right to left, the interference figure will in this case mainly be caused by the X-rays diffracted from the back layer A, and the interference bands on the upper side will be much stronger also than those on the lower side.

Next, in order to test this point still further, the author carried out the experiments with thinner foils, the thickness of which was reduced to about 0·01 m.m. by rolling or by etching with hot aqua-regia. The temperature of the hot aqua-regia used was about 80°C, and it was

confirmed, by taking the photograph of the interference figure, that the arrangement of the micro-crystals in the foil was not affected by heating it merely to this temperature. By etching equally the two rolled surfaces of the foil of 0·04 m.m. in thickness with such hot aqua-regia, the author prepared a foil of about 0·01 m.m. in thickness. The photograph reproduced in Fig. 11 of Plate I was taken with this thin foil by letting the X-rays strike normally the surface of the foil. As is seen from this figure the intensities of the interference bands came out nearly the same now on both sides of the horizontal line. This is in conformity with our previous consideration. Next to reduce the thickness of the sample below 0·04 m.m. by rolling, the author employed another roller of smaller diameter——about 7 cm. Thus, with a foil of about 0·01 m.m. in thickness prepared by rolling, a photograph was also taken under similar circumstances as before. The inequality in intensity of the interference bands nearly disappeared in this case also.

Next, only one side of the sample was etched by hot aqua-regia, and one of the two layers A or B in Fig. 10 was removed. The photographs were taken by projecting the X-ray beam normally to the front or the back surface of the sample, and the writer observed that the difference in the intensities of the upper and the lower parts of the interference figure was very clear, and that the difference in the intensities was now reversed, as is seen in Fig, 12 and Fig. 13, of Plate I according as the direction of projection of the X-rays was from left to right or vice-versa. Fig. 12 of Plate I corresponds to the case in which the beam was projected from the layer A to B, and Fig. 13 of Plate I to the case in which the beam was projected in the opposite direction, the layer B being etched off by hot aqua-regia in both cases. The direction of rolling was upward in both cases as is indicated by the arrow in Fig. 10.

In Fig. 12 of Plate I the interference bands on the lower side of the horizontal line are much stronger than those on the other side, and in Fig. 13 of Plate I this difference in the intensities of the interference bands is reversed. This will be very easily understood from Fig. 10 quite in accordance with our previous consideration.

It has already been stated that the common axis of the micro-crystals in the foil is inclined at about 8° to the direction of rolling. Thus if the X-rays are made to strike the micro-crystals in a direction normal to their common axis by rotating the foil at about 10° about the horizontal line, the inequality in the intensities of the interference bands will no more exist. This was also confirmed to be the case. The photograph reproduced in Fig. 14 of Plate I was taken under such conditions.

Next the writer took photographs in the following two cases:- One, in the case when the sample was placed in a position rotated, from the position of normal incidence, with a proper angle about the direction of rolling; and the other in the case when the sample was placed in a position rotated about the line perpendicular both to the direction of rolling and to that of the incident rays. In the former case, the radiating bands on the side on which the surface of the sample makes an obtuse angle with the direction of the propagation of the X-rays, became longer and some new weak bands appeared, and those on the opposite side became shorter and gradually disappeared as in the previous case. Since the X-rays strike the surface of rolling obliquely, this will be caused partly by the difference in absorption due to the path differences in the foil of the rays diffracted toward the opposite side of the axis of rotation of the foil, and partly by the distribution of the micro-crystals not arranged in their ideal orientation. If we disregard the differences in the intensities of the interference bands and the appearance of some new weak bands, the angular distribution of the radiating bands is seen to be nearly the same as in the case of normal incidence. Fig. 15 of Plate II is reproduced, as an example, to show this point, and the angle of rotation of the sample from the position of the normal incidence of the X-rays was about 30° in this case.

Next let us consider the case when the sample is rotated with a certain angle about the line perpendicular both to the direction of rolling and to that of the X-rays. As is seen from Fig. 10, when the rotation is so made that the angle between the direction of rolling and that of the propagation of the X-rays becomes acute, the angle between the incident beam and the common axis of the micro-crystals in the layer facing the incident beam, will be smaller than that between the incident beam and the direction opposite to that of rolling, and the angle between the incident beam and the common axis of the micro-crystals in the layer facing the emergent beam will be greater than that between the incident beam and the direction opposite to that of rolling. When the rotation of the sample is made in the opposite direction, these differences in inclinations will be reversed. The angle between the direction of rolling and the common axis of the micro-cryatals is about 10° as was stated before; therefore, when the direction of rolling makes an angle of 45° with the direction of the propagation of the X-rays, the common axis in one layer will incline 35° to the incident beam and that in the other layer will incline 55° to the incident beam.

By putting $\alpha=55^\circ$ and $\alpha=35^\circ$ and by giving various values to ϕ,

Table 7.

The values of θ $(\alpha = 55°)$.

Planes	β \ Φ	60°	70°	80°	90°	100°	110°	120°
001	35° 20′	10°	16°	22°	28°	35°	42°	50°
010	65° 55′	4°	6°	13°	20°	26°	29°	30°
100	65° 55′	79°	73°	64°	55°	45°	35°	24°
110	54° 45′	48°	37°	28°	19°	11°	3°	4°
$\bar{1}10$	90°	40°	48°	53°	55°	53°	48°	40°
101	30°	55°	61°	64°	65°	64°	61°	55°
$\bar{1}01$	73° 15′	35°	29°	22°	14°	5°	4°	15°
011	30°	10°	7°	6°	5°	6°	7°	10°
$0\bar{1}1$	73° 15′	5°	15°	25°	35°	45°	55°	64°
111	19° 20′	45°	41°	37°	33°	29°	26°	22°
$1\bar{1}1$	61° 50′	39°	50°	60°	70°	80°	84°	76°
$\bar{1}11$	61° 50′	25°	27°	26°	23°	19°	13°	5°
$11\bar{1}$	90°	30°	20°	10°	0°	10°	20°	30°

Table 8.

The values of θ $(\alpha = 35°)$.

Planes	β \ Φ	60°	70°	80°	90°	100°	101°	120°
001	35° 20′	22°	28°	35°	42°	50°	60°	74°
010	65° 55′	25°	12°	3°	4°	9°	11°	9°
100	65° 55′	55°	59°	55°	48°	39°	28°	14°
110	54° 45′	62°	49°	38°	28°	19°	11°	4°
$\bar{1}10$	90°	16°	27°	33°	35°	33°	27°	16°
101	30°	58°	70°	80°	90°	80°	70°	59°
$\bar{1}01$	73° 15′	18°	16°	10°	3°	6°	17°	30°
011	30°	35°	29°	26°	25°	26°	29°	35°
$0\bar{1}1$	73° 15′	2°	11°	22°	32°	41°	48°	52°
111	19° 20′	70°	62°	56°	51°	46°	41°	37°
$1\bar{1}1$	61° 50′	27°	40°	51°	59°	63°	61°	52°
$\bar{1}11$	61° 50′	1°	6°	7°	5°	0°	7°	19°
$11\bar{1}$	90°	30°	20°	10°	0°	10°	20°	30°

the writer calculated the value of θ, for various reflecting atomic planes of the crystal, by using equations (6) and (5) in the previous report. The results of calculation are tabulated in Table 7 and Table 8. The faces from

Fig. 16.

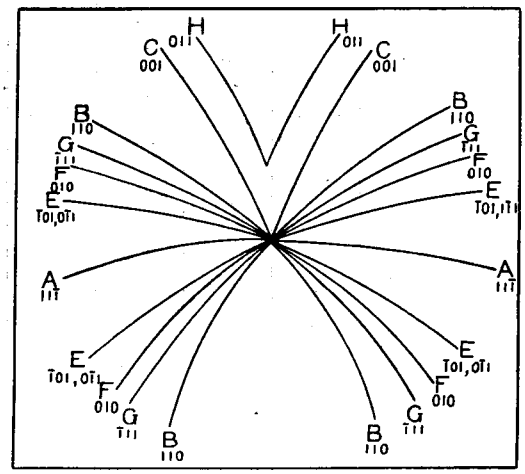

Fig. 17.

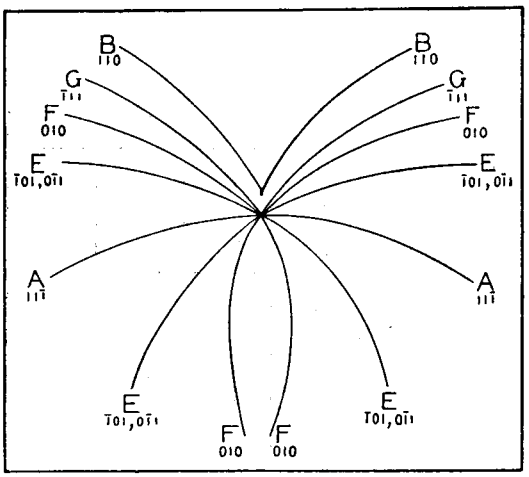

which the reflection will occur were selected by picking out the small values of θ in these Tables, and the interference figures caused by these reflecting planes are represented graphically in Fig. 16 and Fig. 17.

The photograph reproduced in Fig. 18 of Plate II shows the case when the sample was rotated 45°, so that the direction of rolling made an

angle of 45° with the direction of propagation of the X-rays. The position of the spectral lines is not clearly seen, but the angular distribution of the radiating bands is nearly the same as that of the curves represented in Fig. 16. This is to be expected from our previous consideration, if we consider that the more predominant X-rays are those diffracted from the crystals in the back layer of the sample, because the common axis in that layer makes an angle of 55° with the incident beam.

Though the photograph reproduced in Fig. 18 of Plate II is nearly the same as the theoretical drawing of curves shown in Fig. 16, it is not exactly the same. Perhaps this may be due to the fact that the interference bands produced by diffraction from the other layer also appear in the photograph.

On the contrary when the sample was rotated 45° to the opposite direction, the photograph reproduced in Fig. 19 of Plate II was obtained. In this case the angular distribution of the interference bands was nearly the same as that of the curves drawn in Fig. 17, in conformity with our expectation.

In conclusion the author wishes to express his sincere thanks to Prof. Yoshida for his kind guidance.

Plate I.

Fig. 1.

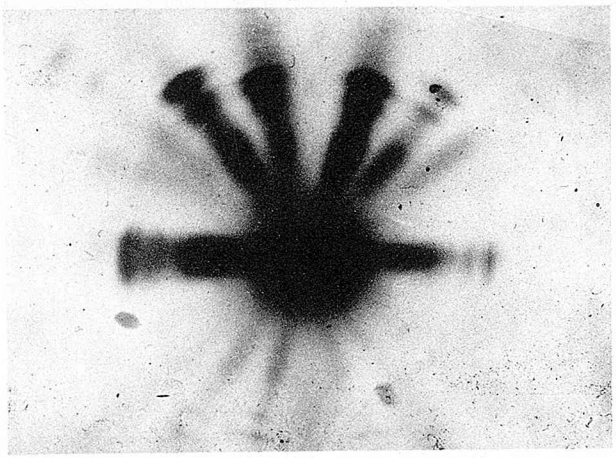

Fig. 11.

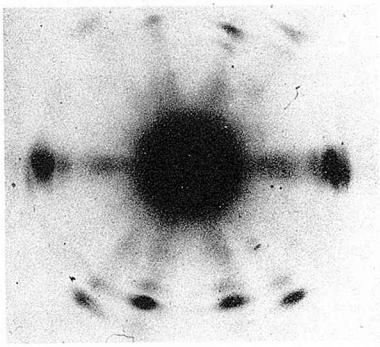

Fig. 12.

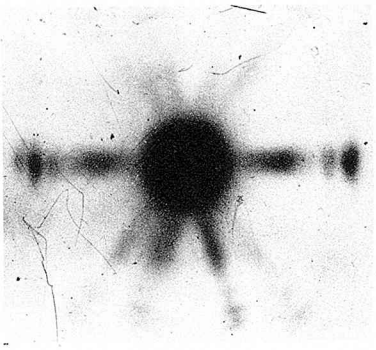

Fig. 14.

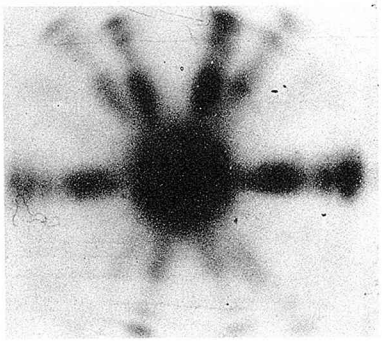

Fig. 13.

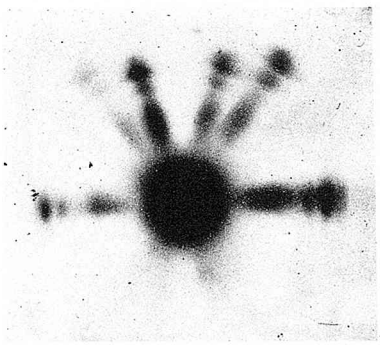

Plate II.

Fig. 15.

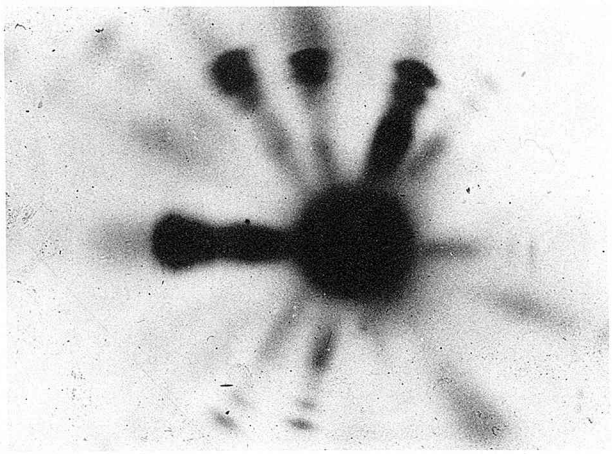

Fig. 18.

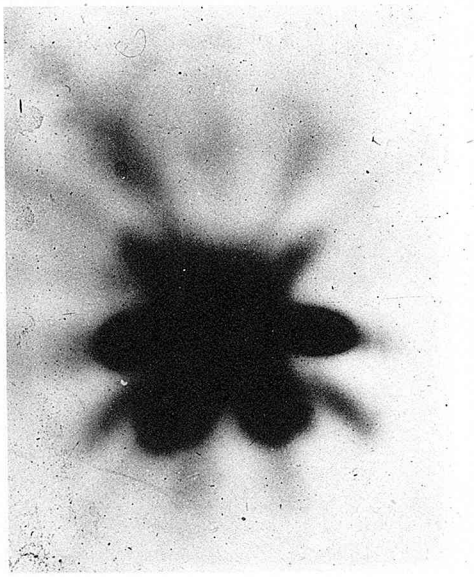

Fig. 19.